The 8th European Congress on Computational Methods in Applied Sciences and Engineering
ECCOMAS Congress 2022
5 – 9 June 2022, Oslo, Norway

NEW PREDICTIVE MODELS FOR BALLISTIC LIMIT OF SPACECRAFT HONEYCOMB-CORE SANDWICH PANELS SUBJECTED TO HYPERVELOCITY IMPACT

RILEY CARRIERE*, ALEKSANDR CHERNIAEV†

* Department of Mechanical, Automotive and Materials Engineering, University of Windsor, 401 Sunset Ave., Windsor N9B 3P4, Canada, carrierr@uwindsor.ca

† Department of Mechanical, Automotive and Materials Engineering, University of Windsor, 401 Sunset Ave., Windsor N9B 3P4, Canada, aleksandr.cherniaev@uwindsor.ca

Key words: Orbital Debris, Hypervelocity Impact, Honeycomb-Core Sandwich Panel, Ballistic Limit Model, Artificial Neural Network

Abstract. Parameters of the honeycomb core (such as cell size and foil thickness), as well as the material of the core, influence the ballistic performance of honeycomb-core sandwich panels in cases of hypervelocity impact (HVI) by orbital debris. Two predictive models capable of accounting for this influence have been developed in this study: one utilized a conventional approach based on a dedicated ballistic limit equation, while the other employed an artificial neural network trained to predict the outcomes of HVI on HCSP. BLE fitting and ANN training were conducted using a database composed of 46 numerical experiments, performed with a validated numerical model and ten physical tests derived from the literature.

The new ballistic limit equation is based on the Whipple shield BLE, in which the standoff distance between the facesheets was replaced by a function of the honeycomb cell size, foil thickness, and yield strength of the HC material. The corresponding fit factors were determined by minimizing the sum of squared errors between the BLE predictions and the results of HVI tests listed in the database. The BLE was then tested against a new set of simulation data and demonstrated an excellent predictive accuracy, with the discrepancy ranging from 1.13% to 5.58% only.

The artificial neural network was developed using MATLAB's Deep Learning Toolbox framework and was trained utilizing the same HCSP HVI database as was employed for the BLE fitting. The ANN demonstrated a very good predictive accuracy, when tested against a set of simulation data not previously used in the training of the network, with the discrepancy ranging from 0.67% to 7.27%.

Both of the developed predictive models (the BLE and the ANN) are recommended for use in the design of orbital debris shielding for spacecraft, involving honeycomb-core sandwich panels.

1 INTRODUCTION

To ensure mission success, Earth satellites must be analysed for their ability to survive hypervelocity impacts (HVI) by orbital debris, as a collision of a functional satellite with even

a millimetre-sized object, traveling at a typical orbital speed (7 km/s and higher), can be detrimental for both the spacecraft and the Earth's orbit environment [1].

In a typical satellite design, most impact-sensitive equipment is situated in the enclosure of the structural honeycomb-core sandwich panels (HCSP). Being the most commonly used elements of satellite structures, these panels form the satellite's shape and are primarily designed to resist launch loads and provide attachment points for satellite subsystems [2]. With low additional weight penalties, their intrinsic ballistic performance can often be upgraded to the level required for orbital debris protection [3]. On the other hand, perforation of a structural honeycomb panel can be considered as a failure criterion, as otherwise unprotected satellite components (e.g., circuit boards, cables) may be rendered non-functional post-impact or even experience catastrophic failure (e.g., pressurized propellant tanks, gas accumulators). Therefore, assessing the orbital debris impact survivability of unmanned satellites requires HVI testing or reliable predictive models for honeycomb-core sandwich panels, capable of accounting for various impact conditions and panel design parameters.

Several such HCSP-specific models (implemented in the form of ballistic limit equations) have been described in the literature. They all stem from the well-known BLE for a Whipple shield. As illustrated in Fig. 1 (left), this commonly used protective system represents a structure consisting of two thin facesheets (walls) separated by some distance, such that the front facesheet fragments the hypervelocity projectile. The empty spacing between the facesheets allow the formed fragment cloud to expand while travelling between the facesheets and, thus, distribute energy and momentum on a wider area of the rear facesheet. The function of the rear facesheet is to collect and stop the shattered projectile fragments.

The Whipple shield BLE for projectile speeds $v_p \geq 7$ km/s is given by following equation [4]:

$$D_{cr} = 3.918 \cdot \sqrt[3]{\frac{\bar{S}}{\rho_p \sqrt[3]{\rho_b}} \cdot \left(\frac{t_{FC}}{v_p \cdot \cos\theta}\right)^2 \cdot \left(\frac{\sigma_{Y,FC}}{70}\right)} \qquad (1)$$

Here: ρ_p and ρ_b are the projectile and front facesheet ('bumper') densities in g/cm^3; t_{FC} – thickness of the rear facesheet in mm; v_p – projectile speed in km/s; θ – impact angle measured from target normal, deg ($\theta = 0$ for normal impact); $\sigma_{Y,FC}$ – facesheet yield strength in ksi; and $\bar{S}$ is a standoff distance between the facesheets, in mm when t_{FC} is also in mm.

For the HCSP, the presence of honeycomb between facesheets has a two-fold effect on the ballistic performance. In the case of oblique impacts, honeycomb walls serve as additional layers that can contribute to the fragmentation of the hypervelocity projectile, thus reducing damage to the rear wall. However, in the case of a normal impact, honeycomb is known to constrain the radial expansion of the fragment cloud, channeling the fragments through its cells [5]. In turn, this results in focusing the impact energy and momentum of the fragments onto a small area of the rear facesheet, as shown in Fig. 1 (right), and facilitates its perforation [6-8]. This most conservative scenario (impact at normal incidence) is usually considered as the design case for orbital debris shielding involving HCSP.

It follows from the above that the ballistic performance of HCSP in case of HVI will be influenced by the parameters of the honeycomb core, such as cell size and foil thickness (see Fig. 1), as well as the material of the core [4, 9]. Together, these affect the severity of fragment channeling. This is in line with the findings of Kang et al. [10] who, through a series of numerical

simulations, concluded that the HC core cell size is the most influential parameter for the damage of the rear facesheet due to the channeling effect. The same conclusions, regarding the HC cell size effect, were reached by Ilescu et al. [11] and Schubert et al. [12].

Sennett and Lathrop [13] proposed a method to account for the cell size effect by replacing standoff distance $\bar{S}$ in (1) by either the product of twice the honeycomb cell size (A_{cell}) or by the core depth (t_{HC}), whichever is less:

$$\bar{S} = \min(2 \cdot A_{cell}, t_{HC}) \qquad (2)$$

This approach, however, is considered to be a 'rough estimate' [4] and does not include other influential parameters, such as foil thickness and material of the core.

The purpose of this study was to develop and validate honeycomb core parameters sensitive BLE and another model – an artificial neural network (ANN) for spacecraft sandwich panels subjected to HVI. The developed predictive models were focused on the most conservative scenario of HVI at the normal incidence and limited to aluminum HCSP.

2 HVI DATABASE

The development of such predictive models – a BLE and an ANN – relied on the availability of a database for HVI on HCSP. Such a database was constructed by combining the results of new numerical simulations conducted in this study with the experimental data already available in the literature.

While a significant amount of experimental data is available for HVI on HCSP [9], the following criteria were used when selecting the experiments suitable for the development of new BLE:

- the projectile impacts the panel at a normal incidence;
- the projectile, the facesheets and the honeycomb core are made of aluminum alloys;
- the data set contains full information about the honeycomb core used, including the cell size and the foil thickness;
- no additional protective elements, such as multilayer insulation (MLI), are involved.

This resulted in a database only containing the ten entries. Among them, only two pairs of tests clearly defined the ballistic limit of the panels used in those experiments. Apparently, although the availability of these experimental results is extremely useful, the database requires a significant extension to be suitable for the derivation of a BLE capable of accounting for the influence of honeycomb core parameters.

To facilitate the creation of a database needed for the development of predictive models, this study adopted the LS-DYNA simulation model that was developed and thoroughly validated in [14] and [15]. The model employed SPH particles to represent a hypervelocity projectile and a front facesheet of a HCSP; shell finite elements (FE) for the representation of a honeycomb core; and adaptive SPH-FE technique for modeling of a rear facesheet, as illustrated in Fig. 1. The model was used to extend the existing experimental database and supplement it with HVI results corresponding to different

- honeycomb cell sizes (3.18 mm [1/8 in], 4.76 mm [3/16 in], and 6.35 mm [1/4 in]),
- honeycomb foil thicknesses (0.025 mm [0.001 in], and 0.075 mm [0.003 in]),
- front and rear facesheet thicknesses (1.0 mm and 1.6 mm), and
- honeycomb depths (25 mm and 50 mm).

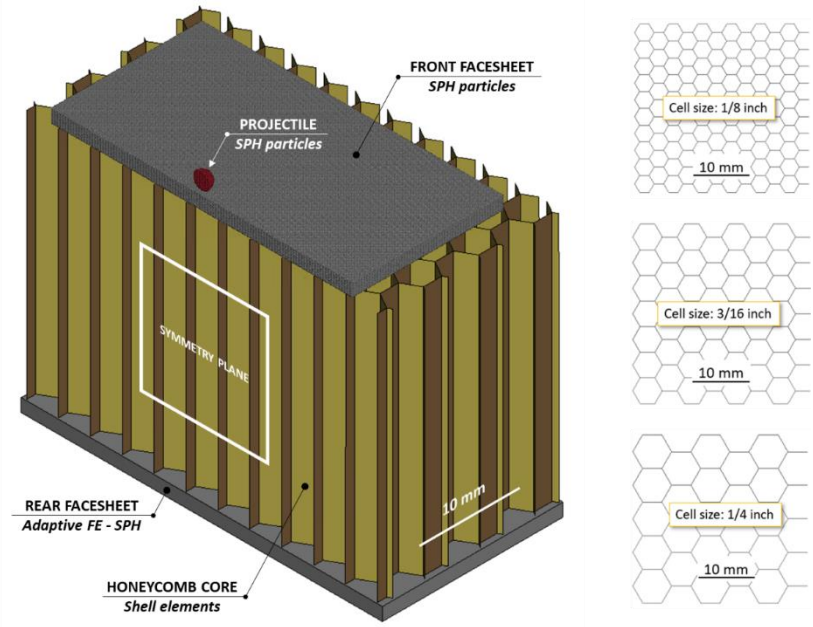

Figure 1: The LS-DYNA model used to simulate HVI on HCSP

A set of 46 simulations was conducted to expand the database available for the new BLE development to 56 entries – experimental and numerical results combined. Different panel configurations and their respective ballistic limits, derived from this database, are summarized in Table 1.

Table 1: Ballistic limits of HCSP configurations considered in physical experiments and numerical simulations

	PROJECTILE		FACESHEETS		HONEYCOMB		BALLISTIC LIMIT
Designation	Speed, km/s	Material	Material	Thickness, mm	Grade*	Depth, mm	D_{cr}, mm
HITF03145	6.80	Al2017-T4	Al6061-T6	0.41	1/8-5052-0.003	12.7	0.90
A	6.75	Al2017-T4	Al7075-T6	1.60	3/16-5056-0.001	50.0	1.71
SIM01	7.00	Al2017-T4	Al6061-T6	1.60	1/8-5052-0.001	25.0	1.70
SIM02	7.00	Al2017-T4	Al6061-T6	1.60	3/16-5052-0.001	25.0	2.50
SIM03	7.00	Al2017-T4	Al6061-T6	1.60	1/4-5052-0.001	25.0	2.50
SIM04	7.00	Al2017-T4	Al6061-T6	1.60	1/8-5052-0.003	25.0	1.50
SIM05	7.00	Al2017-T4	Al6061-T6	1.60	3/16-5052-0.003	25.0	1.90
SIM06	7.00	Al2017-T4	Al6061-T6	1.60	1/4-5052-0.003	25.0	2.10
SIM07	7.00	Al2017-T4	Al6061-T6	1.00	1/8-5052-0.001	50.0	1.10
SIM08	7.00	Al2017-T4	Al6061-T6	1.00	3/16-5052-0.001	50.0	1.30
SIM09	7.00	Al2017-T4	Al6061-T6	1.00	1/4-5052-0.001	50.0	1.50
SIM10	7.00	Al2017-T4	Al6061-T6	1.00	1/8-5052-0.003	50.0	1.10

SIM11	7.00	Al2017-T4	Al6061-T6	1.00	3/16-5052-0.003	50.0	1.10
SIM12	7.00	Al2017-T4	Al6061-T6	1.00	1/4-5052-0.003	50.0	1.30
SIM13	7.00	Al2017-T4	Al6061-T6	1.60	1/8-5052-0.001	50.0	1.50
SIM14	7.00	Al2017-T4	Al6061-T6	1.60	3/16-5052-0.001	50.0	1.90
SIM15	7.00	Al2017-T4	Al6061-T6	1.60	1/4-5052-0.001	50.0	2.30
SIM16	7.00	Al2017-T4	Al6061-T6	1.60	1/8-5052-0.003	50.0	1.50
SIM17	7.00	Al2017-T4	Al6061-T6	1.60	3/16-5052-0.003	50.0	1.70
SIM18	7.00	Al2017-T4	Al6061-T6	1.60	1/4-5052-0.003	50.0	2.10

3 NEW BALLISTIC LIMIT EQUATION

The new BLE for HVI on HCSP proposed in this study is a modification of the Whipple shield BLE, given by (1). The latter can be re-written for the case of normal impacts (the only incidence considered in this study, as discussed earlier) in the following form:

$$D_{cr} = 3.918 \cdot \sqrt[3]{\frac{\bar{S}}{\rho_p \sqrt[3]{\rho_b}} \cdot \left(\frac{t_{FC}}{v_p}\right)^2 \cdot \left(\frac{\sigma_{Y,FC}}{70}\right)} \qquad (3)$$

Here: ρ_p and ρ_b are the projectile and front facesheet ('bumper') densities in g/cm^3; t_{FC} – thickness of the rear facesheet in mm; v_p – projectile speed in km/s; $\sigma_{Y,FC}$ – facesheet yield strength in ksi; and $\bar{S}$ is a standoff distance between the facesheets in the original Whipple shield BLE (in mm when t_{FC} is in mm) and, as proposed by Lathrop and Sennett [13], can be replaced in the case of HCSP by twice the honeycomb cell size (A_{cell}) if it is larger than the distance between facesheets, i.e. $\bar{S} = K \cdot A_{cell}$, where $K = 2.00$.

The BLE proposed in this study does not alter the general expression provided by (3), however the expression for $\bar{S}$ in our BLE was supplemented by additional terms, such that

$$\bar{S} = K \cdot A_{cell} \cdot \left(\frac{t_{HC}}{t_{FC} + \alpha}\right)^{\beta} \cdot \left(\frac{t_{HC}}{t_{foil}}\right)^{\gamma} \cdot \left(\frac{30}{\sigma_{Y,HC}}\right)^{\delta} \qquad (4)$$

where t_{HC} – honeycomb depth in mm; t_{FC} – thickness of a facesheet in mm; t_{foil} – thickness of the honeycomb foil in mm; $\sigma_{Y,HC}$ – yield strength of the honeycomb material in ksi (e.g. 30 ksi for Al5052 and 50 ksi for Al5056 honeycomb); and K, α, β, γ, δ are parameters with the values given in Table 2 below.

Table 2: Parameters of the new HCSP BLE

BLE parameter	K	α	β	γ	δ
Value	2.63	1.893	-0.804	0.304	1.915

The new BLE fit factors presented in Table 2 were determined by minimizing the discrepancy (expressed in terms of the sum of squared errors, SSE) between the BLE predictions and the experimental or simulation data provided in Table 1 (ballistic limits summary). The goodness-of-fit diagrams for the Whipple shield BLE with the Lathrop and Sennett correction for the honeycomb core effect ($S = 2A_{cell}$) and the BLE proposed in this

study, are shown in Fig. 2. BLE predictions for the outliers are added as data labels on the goodness-of-fit diagrams. As can be deduced from Fig. 3, the new BLE provides a significant improvement in terms of the predictive accuracy, compared to the Whipple shield BLE with the Lathrop and Sennett correction.

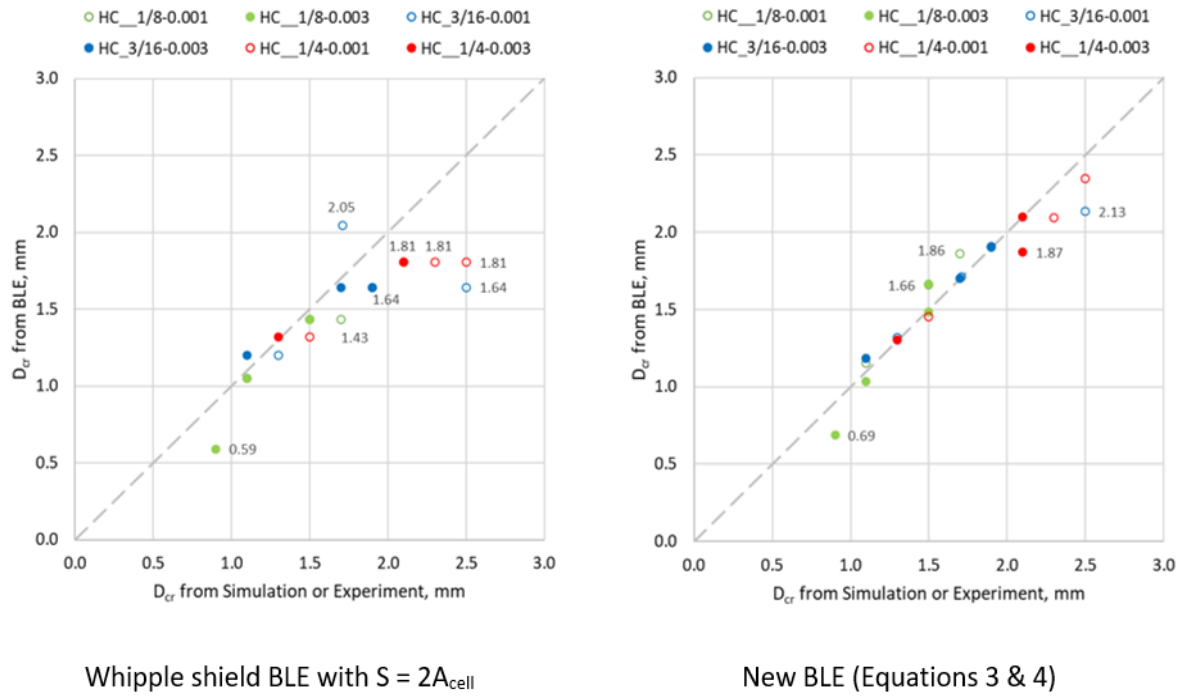

Figure 2: Goodness of fit diagrams for the Whipple shield (with Sennett-Lathrop correction) and the new BLE

4 ARTIFICIAL NEURAL NETWORK

MATLAB's Deep Learning Toolbox was used to develop an ANN capable of predicting perforating/non-perforating outcomes of HVI of all-aluminum HCSP structures and projectiles at normal incidence. A binary output classification scheme was established with the pass 'non-perforating' and fail 'perforating' classes set. A perforating case is defined as being when the fragments fully penetrate through the rear facesheet.

Neural network architecture consisted of an input layer, one hidden layer and an output layer. Here, the input layer contains the projectile description (projectile size and material), panel description (facesheet and core thicknesses and material, core foil thickness and cell size) and impact parameters (impact incidence angle and projectile speed).

Input data is passed to the neurons/nodes located within the hidden layer, which assess the data versus a set criterion defined by the activation function. When assessed, there are two possible outcomes: if the input criteria satisfy the conditions set, the neuron/node is activated; if not, then there is no activation. Activations are calculated using the weighted sums and associated bias of each neuron/node. Each neuron/node has adjustable weightings assigned in a similar fashion to the coefficients used in BLE tuning and curve fitting, which are optimized to improve predictive accuracy. The accumulation of the neurons/nodes, associated weightings and activation functions create a hidden layer.

Outputs from the hidden layer are passed off to the output layer, the output layer then assigns

a classification of perforating or non-perforating to each instance predicted, as determined from its own activation function and neuron/node analysis.

The ANN training database in this study was composed of the experimental and numerical tests presented in the HCSP HVI database. Training sets were established using a hold-out validation scheme, using 80% of the database (44 entries, randomly selected), for the ANN to learn and develop relations. Once developed, the remaining 20% of the database located in the testing set (12 entries), were used as 'true' prediction scenarios, allowing for analysis of the ANN's predictive accuracy against known outcomes in the database.

5 VERIFICATION OF THE PREDICTIVE MODELS

To conduct verification of the developed predictive models (new BLE and ANN), additional numerical simulations were performed and their results were compared with the BLE and ANN predictions. It should be noted that these new datapoints have not been used in either BLE fitting or ANN training and, thus, were 'unfamiliar' to both predictive models. Also, panel configurations in these additional numerical simulations featured one or multiple design parameters which have not been represented in the database used for BLE fitting and ANN training.

Table 3 compares the ballistic limit predictions of the new BLE, ANN and the verified LS-DYNA model. As can be deduced from the table, in all cases, the BLE demonstrated an excellent correlation with the predictions of the sophisticated numerical model, with the discrepancy ranging from 1.13% to 5.58% only. For the ANN, ballistic limit estimations of impact scenarios VER01 to VER05 were iteratively determined using the ANN to classify outputs for critical projectile diameters until the ballistic limit was sandwiched between a passing (non-perforating) and failing (perforating) outcome. Critical projectile diameter estimations by the ANN closely resembled the simulation ballistic limits: the difference between simulation and ANN predictions ranged between 0.67% and 7.27%.

Table 3: Verification of BLE and ANN predictions

	PROJECTILE		FACESHEETS		HONEYCOMB		BALLISTIC LIMIT		
Designation	Speed, km/s	Material	Material	Thickness, mm	Grade*	Depth, mm	D_{cr}, mm		
							SIM	BLE	ANN
VER01	7.00	Al2017-T4	Al6061-T6	1.30	1/8-5052-0.001	25.0	1.50	1.58	1.53
VER02	7.00	Al2017-T4	Al6061-T6	1.60	3/16-5052-0.003	38.0	1.70	1.78	1.76
VER03	7.00	Al2017-T4	Al6061-T6	1.00	5/32-5052-0.002	50.0	1.10	1.16	1.18
VER04	7.00	Al2017-T4	Al6061-T6	1.30	5/32-5052-0.002	38.0	1.50	1.48	1.51
VER05	7.00	Al2017-T4	Al7075-T6	1.00	1/4-5056-0.001	50.0	1.30	1.26	1.26

6 CONCLUSIONS

The new ballistic limit equation developed in this study is based on the Whipple shield BLE, in which the standoff distance between the facesheets was replaced by a function of the honeycomb cell size, foil thickness, and yield strength of the HC material. The corresponding fit factors were determined by minimizing the sum of squared errors between the BLE

predictions and the results of HVI tests listed in the database. The BLE was then tested against a new set of simulation data and demonstrated an excellent predictive accuracy, with the discrepancy ranging from 1.13% to 5.58% only.

The artificial neural network was developed using MATLAB's Deep Learning Toolbox framework and was trained utilizing the same HCSP HVI database as was employed for the BLE fitting. The ANN demonstrated a very good predictive accuracy, when tested against a set of simulation data not previously used in the training of the network, with the discrepancy ranging from 0.67% to 7.27%.

Both of the developed predictive models (the BLE and the ANN) are recommended for use in the design of orbital debris shielding for spacecraft, involving honeycomb-core sandwich panels.

REFERENCES

[1] Pelton J., Space Debris and Other Threats from Outer Space. Springer, 2013.

[2] Bylander, L. A., O. H. Carlström, T. S. R. Christenson, and F. G. Olsson. 2002. "A Modular Design Concept for Small Satellites". In Smaller Satellites: Bigger Business?, 357–58. Springer Netherlands.

[3] Cherniaev A., Telichev I. (2016). Weight-Efficiency of Conventional Shielding Systems in Protecting Unmanned Spacecraft from Orbital Debris. Journal of Spacecraft and Rockets. 54(1): 75-89.

[4] Christiansen, E.L. et al. (2009). Handbook for Designing MMOD Protection. NASA JSC-64399, Version A, JSC-17763.

[5] Deconinck, P., Abdulhamid, H., Héreil, P. L., Mespoulet, J., & Puillet, C. (2017). "Experimental and numerical study of submillimeter-sized hypervelocity impacts on honeycomb sandwich structures". Procedia engineering, 204, 452-459.

[6] Taylor, E. A., Herbert, M. K., Vaughan, B. A. M., & McDonnell, J. A. M. (1999). Hypervelocity impact on carbon fibre reinforced plastic/aluminium honeycomb: comparison with Whipple bumper shields. International Journal of Impact Engineering, 23(1), 883-893.

[7] Taylor, E., Herbert, M., & Kay, L. (1997). Hypervelocity Impact on Carbon Fibre Reinforced Plastic (cfrp)/aluminium Honeycomb at Normal and Oblique Angles. In Second European Conference on Space Debris (Vol. 393, p. 429).

[8] Taylor, E. A., Herbert, M. K., Gardner, D. J., Kay, L., Thomson, R., & Burchell, M. J. (1997). Hypervelocity impact on spacecraft carbon fibre reinforced plastic/aluminium honeycomb. Proceedings of the Institution of Mechanical Engineers, Part G: Journal of Aerospace Engineering, 211(5), 355-363.

[9] Carriere, R., & Cherniaev, A. (2021). Hypervelocity Impacts on Satellite Sandwich Structures—A Review of Experimental Findings and Predictive Models. Applied Mechanics, 2(1), 25-45.

[10] P. Kang, S. K. Youn, and J. H. Lim (2013). Modification of The Critical Projectile Diameter of Honeycomb Sandwich Panel Considering The Channeling Effect in Hypervelocity Impact, Aerosp. Sci. Technol., 29(1), pp. 413–425.

[11] Iliescu, L. E. Lakis, A. A. & Oulmane, A (2017). Sattelites/Spacecraft Materials And Hypervelocity Impact (HVI) Testing: Numerical Simulations, Journal, M. Engineering, E. Centre, and D. Uk, 4 (1), pp. 24–64.
[12] M. Schubert, S. Perfetto, A. Dafnis, D. Mayer, H. Atzrodt, K. U. Schroder (2017) Multifunctional Load Carrying Lightweight Structures For Space Design, Institute of Structural Mechanics and Lightweight Design, RWTH Aachen University, Fraunhofer Institute for Structural Durability and System Reliability LBF , Darmstadt, pp. 1–11.
[13] B. Lathrop, and R. Sennett (1968). The Effects of Hypervelocity Impact on Honeycomb Structures", In 9 th Structural Dynamics and Materials Conference. American Institute of Aeronautics and Astronautics.
[14] R. Aslebagh, A. Cherniaev (2022). Projectile Shape Effects in Hypervelocity Impact of Honeycomb-Core Sandwich Structures. J. Aerosp. Eng., 35(1).
[15] R. Carriere, A. Cherniaev (2022). Honeycomb Parameter-Sensitive Predictive Models for Ballistic Limit of Spacecraft Sandwich Panels Subjected to Hypervelocity Impact at Normal Incidence. J. Aerosp. Eng., 35(4).